ELSEVIER

Polymer 42 (2001) 7197–7202

polymer

www.elsevier.nl/locate/polymer

Polymer Communication

Experimental evidence of the glass transition in a metallocene ethylene-1-octene copolymer and its composites with glass fibre

María L. Cerrada[a,*], Rosario Benavente[a], Ernesto Pérez[a],
Jorge Moniz-Santos[b], M. Rosario Ribeiro[b]

[a]*Instituto de Ciencia y Tecnología de Polímeros (CSIC), Juan de la Cierva 3, 28006 Madrid, Spain*
[b]*Instituto Superior Técnico, Av. Rovisco Pais, 1049-001 Lisboa, Portugal*

Received 8 January 2001; received in revised form 7 March 2001; accepted 13 March 2001

Abstract

Experimental evidence is reached by differential scanning calorimetry (DSC), and modulated differential scanning calorimetry (MDSC), about the existence of a glass transition in a commercial ethylene-1-octene copolymer synthesized with a metallocene catalyst and in its corresponding composites with glass fibre at different content of reinforcement. The glass transition is found in the region from −50 to −45°C depending upon the empirical protocol. Its location is quite independent on the fibre content. The presence of reinforcement in the polymeric matrix has some influence on the crystalline regions, since slightly more perfect crystals seem to be obtained in the composites with not very high glass fibre content, judging from the better resolution of the (110) diffraction and from the slightly higher melting temperatures. However, the normalized crystallinity remains practically unchanged in all the samples. © 2001 Elsevier Science Ltd. All rights reserved.

Keywords: Differential scanning calorimetry; Modulated differential scanning calorimetry; Glass transition

1. Introduction

When dealing with the relaxation spectrum of semicrystalline polymers, the glass–rubber relaxation arising from the amorphous fraction can be easily identified in most cases, specially in those where it is possible to obtain completely amorphous specimens. Thus, it corresponds usually with the β process in such spectrum (or α_a relaxation, the notation depending on the presence or absence of a crystalline phase dependent α relaxation). This relaxation is much broader and the relaxed modulus is displaced dramatically upward in the semicrystalline polymers but it is nevertheless directly traceable to a glass–rubber relaxation that occurs when the material is in the completely amorphous state. In addition, other relaxation processes, depending on the polymer structure, may occur at lower temperatures in these polymers whether in the semicrystalline or completely amorphous state (and they are largely or completely resident in the amorphous fraction when semicrystalline).

In the case of polyethylene, however, the assignment of the glass transition to the γ or β relaxations has been a matter of continued intensive study as well as widespread disagreement [1–6]. On the one hand, some authors, based on experiments of ^{13}C Nuclear Magnetic Resonance, concluded that the β process could not be identified with the glass transition in either branched or linear polyethylene. On the other hand, the relative lack of sensitivity to morphological factors (presence or absence of crystalline fraction) and the magnitude of the activation parameters have suggested that the γ relaxation has its origin in relatively localized molecular motions [5]. To designate the γ process as the glass transition in linear polyethylene would be justifiable only if one wishes to describe the more prominent amorphous phase relaxation as the glass transition. Molecular dynamics simulations have predicted a volumetric glass transition in amorphous polyethylene associating the β process with the glass transition [6,7].

The use of metallocene catalysts has allowed to attain ethylene-α-olefin copolymers with a uniform length of the branches, a very random distribution of the comonomer along the backbone, a unique distribution of the comonomer in different chains and a very narrow molecular weight distribution. These characteristics are very convenient for the study of the structure–properties relationships since there is no need to fractionate the samples and the homogeneous distribution of comonomer is a great advantage when studying the properties' dependencies with the

---

* Corresponding author. Tel.: +34-91-5622900; fax: +34-91-5644853.
E-mail address: ictcg26@fresno.csic.es (M.L. Cerrada).

PII: S0032-3861(01)00199-9

composition. Depending upon comonomer content, the metallocene-catalyzed copolymers show three or two relaxation processes [8–11]: γ, β and α in order of increasing temperatures. The γ relaxation is attributed to restricted conformational transitions, as kink formation, inversion and migration of polymethylenic chains [12–15]. Molecular dynamics simulations have been a powerful tool to corroborate the just mentioned nature of these conformational motions underlying this relaxation [7,16]. The β relaxation has been universally detected in branched polyethylenes at temperatures around −20°C, but it sometimes appears, though weakly, in some samples of linear polyethylene. From the study of various polyethylenes and their copolymers, some authors have concluded that this relaxation results from motions of chain units in the interfacial region [17,18] whereas some others attributed this process to the glass transition [5–7]. Finally, the α relaxation has been associated to vibrational and reorientational motions within the crystallites [19,20].

Modulated differential scanning calorimetry (MDSC), is a relatively new technique in thermal analysis in which the normal temperature scan used in differential scanning calorimetry (DSC), is, generally, overlaid by a sinusoidal perturbation. The purported advantages of MDSC include the ability to separate overlapping phenomena, as well as improved resolution and sensitivity. In the MDSC experiments, the modulated heat flow raw data are deconvoluted by Fourier Transform algorithm [21] allowing the calculation of reversing heat flow (caused by the modulation and also known as cyclic component) and total heat flow (caused by the underlying heating rate and corresponding to conventional DSC data). The difference is the non-reversing heat flow, indicating the contribution of all the kinetics' events, which cannot follow the modulation. Empirically it has been found that: (1) the glass transition appears in the total and reversing component of the heat flow; (2) the crystallization process appears in the total and non-reversing component, but not in the reversing component of the heat flow; and (3) the melting process may be visible in all three components of the resolved data [22]. DSC and MDSC have been used to analyse the melting and crystallization of metallocene ethylene-1-octene copolymers [23,24]. These studies have shown that at the glass transition the melting process begins and the crystallization process ends. But none of them have analysed the glass transition process. Therefore, the aim of this work is to investigate either the existence or the location of the glass transition of a commercial metallocene ethylene-1-octene copolymer and its composites with glass fibre by conventional DSC. MDSC is used to assure that this process is certainly a glass transition. In addition, the effect of glass fibre in the diffraction patterns and melting process is discussed.

2. Experimental

A commercial ethylene-1-octene copolymer (CEO) with a 9.27 mol% comonomer content is analysed in the current paper and has been supplied by Exxon Chemical. Chopped strands of E glass fibres of 6 mm long, grade E-11 supplied by Cristalera Española S. A. were utilized in the composites.

Composites with different content in glass fibre: 5, 10, 20 and 40% in weight, labeled as CEOGF5, CEOGF10, CEOGF20 and CEOGF40 respectively, were prepared in a Haake Rheocord 9000 at 150°C and at 40 rpm for 10 min. After blending and homogenization of the two components, sheets specimens were obtained as films by compression molding in a Collin press between hot plates (130°C) at a pressure of 1.5 MPa for 10 min. A quench was applied to the different films from the melt to room temperature.

Wide-angle X-ray diffraction patterns were recorded in the reflection mode at room temperature by using a Philips diffractometer with a Geiger counter, connected to a computer. Ni-filtered CuK_α radiation was used. The diffraction scans were collected over a period of 20 min in the range of 2θ values from 3 to 43 degrees, using a sampling rate of 1 Hz. The goniometer was calibrated with a silicon standard.

Conventional calorimetric analyses were carried out in a Perkin–Elmer DSC7 calorimeter, connected to a cooling system and calibrated with different standards. The sample weights ranged from 6 to 8 mg. A temperature range from −70 to 150°C has been studied and the used heating rates were 20 and 40°C min^{-1}. The value of the glass transition was obtained from the midpoint of the heat capacity change. The reader is referred to Seyler [25] for a discussion of the measurement uncertainties typical of DSC measurements as well as for a discussion of the differences in assignment of T_g values based on different measurement techniques. For crystallinity determinations, a value of 290 J g^{-1} has been taken as the enthalpy of fusion of a perfectly crystalline material [26].

Modulated differential scanning calorimetric experiments were performed on a TA Instruments 2920 MTDSC calorimeter, connected to a liquid nitrogen cooling system and calibrated with different standards. Calibration for heat flow scales was made using indium as reference and checked via heat capacity measurements with a sapphire disc in the range of interest. The sample weights were around 11 mg in all the specimens. The MDSC experiments were performed with a sinusoidal temperature oscillation overlaid on the linear temperature ramp. Preferred modulation parameters are a period of 90 s, an amplitude of 3°C and an underlying heating rate of 2°C min^{-1}. A temperature range from −100 to 0°C has been studied.

3. Results and discussion

Fig. 1 displays the different X-ray patterns found at room temperature for the copolymer CEO and the different composites with distinct glass fibre content. Polyethylene, under usual conditions, crystallizes in the typical orthorhombic lattice [27]. It is evident from Fig. 1 that the

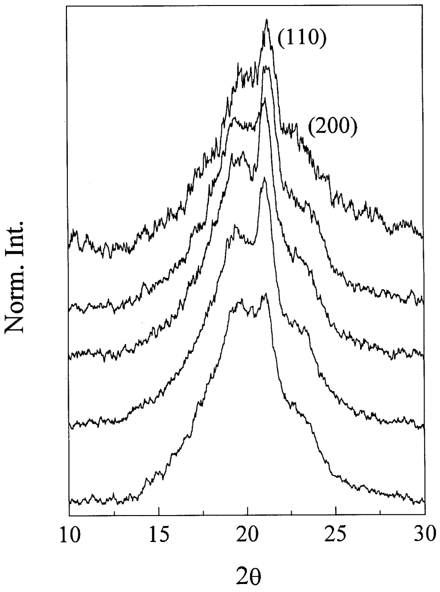

Fig. 1. X-ray diffraction patterns of the different specimens. From top to bottom: CEOGF40Q, CEOGF20Q, CEOGF10Q, CEOGF5Q and CEOQ.

presence of comonomer, 9.27 mol% in 1-octene, leads to a considerable distortion of the polyethylene crystal lattice though the (110) and (200) diffractions peaks of the orthorhombic unit cell are observed in the copolymer CEO. Compared to polyethylene homopolymer, a decrease of the intensity in the (110) diffraction is exhibited and the (200) one becomes a shoulder in the pattern. In addition, diffractions are broadened and shifted to lower angles indicating a diminishment in the crystallites' size and less perfect crystals, respectively. Some studies have shown that, in general, the alkyl branches cannot enter into the polyethylene crystal lattice. Exclusively, the methyl branches are included in the lattice at a substantial degree [28–31] and a small proportion of ethyl ones has been also found in crystalline environments [32,33]. The excluded branches are supposed to be predominantly in the interfacial region. As comonomer content increases, the average number of consecutive ethylene units decreases and the crystallizable part becomes smaller. Consequently, crystallinity decreases as the comonomer content rises in the copolymer [8–11,30]. Moreover, and for high comonomer content, like in the present case, besides the (110) and (200) reflections, a third crystalline reflection, centred at about 4.53Å, is observed [11,24,34]. This reflection is attributed to a hexagonal phase more disordered than the orthorhombic one.

The composites with different glass fibre content exhibit similar diffractograms than the copolymer matrix. However, the introduction of the glass fibre provokes an increase in the intensity of the (110) diffraction suggesting, in some extension, the participation of the fibres on the crystallization process, acting as nucleation centres. This effect is more important up to a glass fibre content of 20%. For the specimen with the highest reinforcement degree, a decrease of the (110) diffraction is observed compared with the other composites although the noise level is much higher, due to the decrease of polymer content. An extensive analysis of the crystallization process is currently being carried out in these composites by SAXS and microscopy.

The glass transition is strongly affected by the presence of crystallites in polymers. The intensity and the breadth of this process are, respectively, smaller and higher than those found in the same system in the amorphous state. Therefore, sometimes glass transition is not easy to be observed by DSC in some semicrystalline polymers, mainly when its location is close to the melting process. In the materials under study, a very broad melting process is exhibited, starting just after T_g. Accordingly, T_g determination by conventional DSC in polyethylene and its α-olefins copolymers might be discussed by authors that postulate its location in a different temperature range considering the change in the heat flow as the initiation of the melting process. As mentioned before, the current work precisely addresses the location of T_g in a copolymer with a high content of 1-octene and its different glass fibre composites.

Fig. 2 shows the conventional DSC traces for the copolymer and the different glass fibre composites, analysed at a heating rate of 20°C min^{-1}. In this Fig. 2, a change in the slope of the heat flow at around −47°C for the different specimens is observed at this heating rate. It could be attributed either to the glass transition of the copolymer or to the beginning of the melting process of the smallest crystallites. This change in the slope is somewhat better resolved when a heating rate of 40°C min^{-1} is used (Fig. 3). Assuming that it

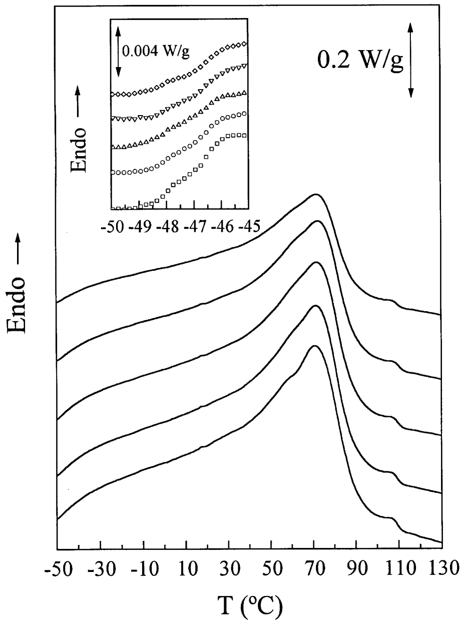

Fig. 2. DSC melting curves corresponding to the copolymer and the different composites at a heating rate of 20°C/min. From top to bottom: CEOGF40Q, CEOGF20Q, CEOGF10Q, CEOGF5Q and CEOQ. In the insert, the glass transition region.

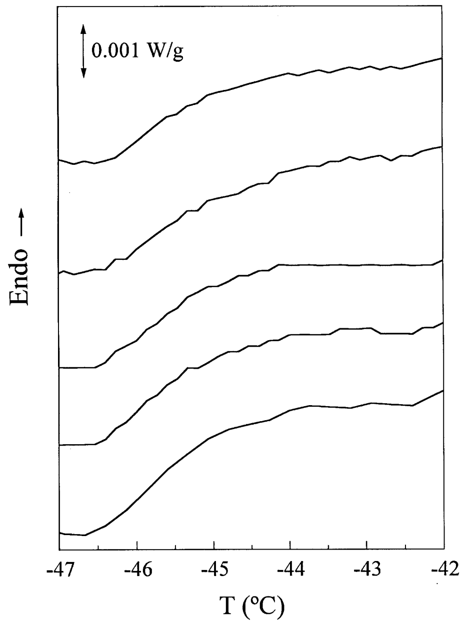

Fig. 3. DSC melting curves in the glass transition region corresponding to the copolymer and the different composites at a heating rate of 40°C/min. From top to bottom: CEOGF40Q, CEOGF20Q, CEOGF10Q, CEOGF5Q and CEOQ.

is a glass transition, the corresponding values of T_g are reported in Table 1. These values indicate that they are quite independent on the introduction of fibre in the matrix.

MDSC is a very useful tool to distinguish the existence of a very weak transition in the conventional calorimeter if the convenient experimental conditions are used. The purpose of using this technique is to corroborate that the thermal step observed in the region of −50 and −40°C is the glass transition of this ethylene-1-octene copolymer (and its corresponding composites with glass fibre). Consequently, a temperature range from −100 to 0°C has been analysed. The choice of correct modulation parameters is a prerequisite to assure steady state. Preliminary experiments have shown that a temperature amplitude of 3°C and a period of 90 s are the best choice and were selected to perform the measurements. It has also been checked that distortion of the heat flow sine wave does not occur under the selected modulation conditions and that a minimum of 5–6 cycles is achieved through the glass transition in order to assure proper separation of the heat flow during the transition.

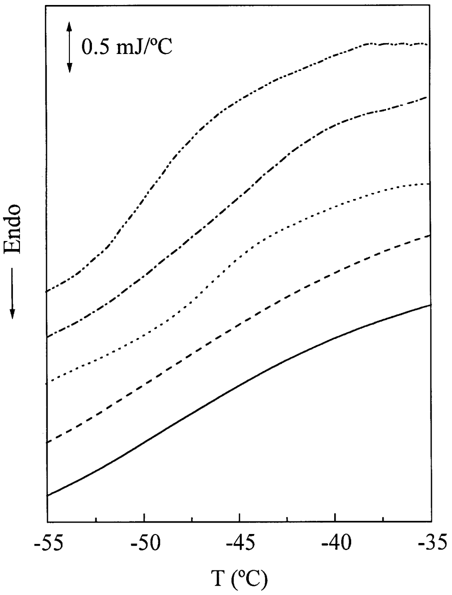

Fig. 4. Complex heat capacity in the glass transition region for the different samples measured by MDSC. From top to bottom: CEOGF40Q, CEOGF20Q, CEOGF10Q, CEOGF5Q and CEOQ.

Fig. 4 shows the results for the complex heat capacity. A clear glass transition is exhibited for the different materials at around −48°C (Table 1). The location of the transition is now slightly dependent on the fibre content. It seems that a glass fibre content up to 20% in weight imposes some hindrances into the amorphous phase and, consequently, the glass transition temperature increases. On the other hand, mobility in the amorphous regions looks easier as reinforcement content is 40% in weight and T_g is slightly shifted to lower temperatures. Fig. 5 displays more evidences that this transition is really the glass transition of these materials. The reversible heat flow, the heat flow phase and the derivative of the complex heat capacity are depicted for the CEO copolymer and the composite with a glass fibre content of 5%. An endothermic transition is observed in the former magnitude, which corresponds to the glass transition of these materials. On the other hand, a minimum and a maximum are found in the plots of the heat flow phase and the derivative complex heat capacity, respectively. Both of them are again an indicative feature that this thermal transition is a glass transition without any doubt.

Table 1
Glass transition temperatures determined from DSC and MDSC measurements and melting temperatures (T_m), enthalpies of melting (ΔH) and crystallinities estimated from DSC

Sample	T_g^{DSC} (°C) at 20°C min^{-1}	T_g^{DSC} (°C) at 40°C min^{-1}	T_g^{MDSC} (°C) from Cp*(mJ/°C)	T_m^{DSC} (°C) at 20°C min^{-1}	ΔH (J/g) at 20°C min^{-1}	f_c^{DSC}
CEOQ	−47.0	−45.5	−49.0	70.8	86	0.30
CEOGF5Q	−47.0	−45.5	−48.5	71.2	84	0.29
CEOGF10Q	−47.0	−45.5	−47.0	71.5	84	0.29
CEOGF20Q	−47.0	−45.5	−47.0	72.0	85	0.29
CEOGF40Q	−47.0	−45.5	−50.0	71.4	86	0.30

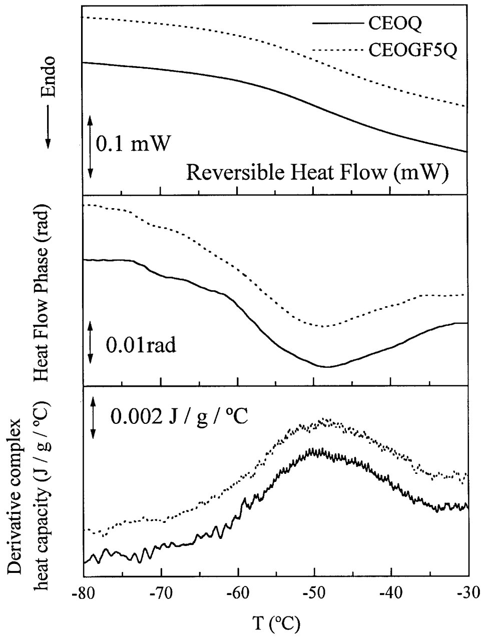

Fig. 5. Reversible heat flow, heat flow phase and derivative of complex heat capacity for the pure copolymer and the composite with a content of glass fibre of 5% in weight.

In addition to the glass transition, Fig. 2 shows the melting process of the crystallites developed in the different structures. The location of the main melting peak is quite independent on the content of reinforcement in the composite. A diminishment of the intensity in the melting curve is observed as glass fibre content is increased in the composite, due to the smaller amount of copolymer in the global material. However, the actual enthalpy of the melting process calculated just from after T_g to 120°C, is similar in all the samples, as reported in Table 1. Accordingly, crystallinity estimated from these DSC experiments, when normalized to the copolymer content in the composites, is similar for all the specimens under study. On the other hand, the melting temperature is shifted to slightly higher temperatures, pointing out the presence of somewhat larger crystallites in the composites. Therefore, although the normalized crystallinity remains practically unchanged, the reinforcement seems to provoke some morphological changes, since more perfect crystals are obtained in the composites with not very high glass fibre content, judging from the better resolution of the (110) diffraction and from the slightly higher melting temperatures. A more detailed study of these possible morphological changes is under way.

4. Conclusions

An experimental evidence of the existence of a glass transition has been reported for a commercial ethylene-1-octene copolymer synthesized with a metallocene catalyst and its composites with glass fibre as reinforcement. Such a glass transition has been observed in the temperature range from −50 to −45°C by conventional DSC and MDSC. The location of such a glass transition is quite independent on the glass fibre content in the composite. The fibre has some influence on the crystalline regions, since slightly more perfect crystals seem to be obtained in the composites with not very high glass fibre content, judging from the better resolution of the (110) diffraction and from the slightly higher melting temperatures. However, the normalized crystallinity remains practically unchanged in all the samples.

Acknowledgements

The financial support of the CAM (Project 07N/0051/1998) and Comisión Mixta CSIC/ICCTI and the supply of the copolymer by EXXON Chemical and of the glass fibres by Cristalera Española S. A. are gratefully acknowledged.

References

[1] Stehling FC, Mandelkern L. Macromolecules 1970;3:342.
[2] Boyer RF. Macromolecules 1973;6:228.
[3] Davis GT, Eby RK. J Appl Phys 1973;44:4274.
[4] Dechter JJ, Axelson DE, Dekmezian A, Glotin M, Mandelkern L. J Polym Sci Polym Phys 1982;20:641–50.
[5] Boyd RH. Macromolecules 1984;17:903–11.
[6] Han J, Gee RH, Boyd RH. Macromolecules 1994;27:7781–4.
[7] Jin Y, Boyd RH. J Chem Phys 1998;108(23):9912–23.
[8] Bensason S, Minick J, Moet A, Chum S, Hiltner A, Baer E. J Polym Sci Polym Phys 1996;34:1301–15.
[9] Simanke AG, Galland GB, Freitas L, da Jornada JAH, Quijada R, Mauler RS. Polymer 1999;40:5489–95.
[10] Cerrada ML, Benavente R, Peña B, Pérez E. Polymer 2000;41:5957–65.
[11] Cerrada ML, Benavente R, Pérez E. J Mater Res 2001.
[12] Schatzki TF. J Polym Sci 1962;57:496.
[13] Boyer RF. Rubb Chem Technol 1963;36:1303–421.
[14] Boyd RH, Breitling RS. Macromolecules 1974;7:855–62.
[15] Boyd RH. J Polym Sci Polym Phys 1975;13:2345–55.
[16] Boyd RH, Gee RH, Han J, Jin Y. J Chem Phys 1994;101(1):788–97.
[17] Popli R, Mandelkern L. Polymer Bull. 1983;9:260–7.
[18] Popli R, Glotin M, Mandelkern L, Benson RS. J Polym Sci Polym Phys 1984;22:407–48.
[19] McCrum NG, Read BE, Williams G. Anelastic and dielectric effects in solid polymers. New York: Dover, 1991.
[20] Ward IM. Mechanical properties of solids polymers. 2nd ed. Chichester: Wiley, 1985. Chap. 8.
[21] Wunderlich B. J Therm Anal 1997;48(2):207–24.
[22] Reading M, Luget A, Wilson R. Thermochim Acta 1994;238(1–2):295–307.
[23] Mathot VBF, Pijpers MFJ. J Appl Polym Sci 1990;39:979–94.
[24] Androsch R. Polymer 1999;40:2805–12.
[25] Seyler RJ, editor. Assignment of the glass transition. Philadelphia, PA: American Society of Testing and Materials, 1994 ASTM STP 1249.
[26] Wunderlich B. Macromolecular physics, 3. New York: Academic Press, 1980. p. 42.
[27] McFaddin DC, Russell KE, Wy G, Heyding RD. J Polym Sci Polym Phys 1993;31(2):175–83.
[28] Alamo R, Domszy R, Mandelkern L. J Phys Chem 1984;88:6587.

[29] Alamo RG, Viers BD, Mandelkern L. Macromolecules 1993;26(21): 5740–7.

[30] Minick J, Moet A, Hiltner A, Baer E, Chum SP. J Appl Polym Sci 1995;58:1371–84.

[31] Shirayama K, Kita S-I, Watabe H. Die Makromol Chem 1972;151:97.

[32] VanderHart DL, Pérez E. Macromolecules 1986;20:1902.

[33] Pérez E, VanderHart DL, Crist Jr B, Howard PR. Macromolecules 1987;21:78.

[34] Androsch R, Blackwell J, Chvalun SN, Wunderlich B. Macromolecules 1999;32:3735–40.